

Propagation lengths of surface plasmon polaritons on metal films with arrays of subwavelength holes by infrared imaging spectroscopy

Katherine E. Cilwa, Kenneth R. Rodriguez, Joseph M. Heer, Marvin A. Malone, Lloyd D. Corwin, and James V. Coe^{a)}

Department of Chemistry, The Ohio State University, 100 West 18th Avenue, Columbus, Ohio 43210-1173, USA

(Received 26 May 2009; accepted 23 July 2009; published online 12 August 2009)

Metal films with arrays of subwavelength holes (mesh) exhibit extraordinary transmission resonances to which many attribute a role for surface plasmon polaritons (SPPs); others debated this point. Experimental measurements of propagation lengths are presented under conditions that pertain to the use of SPPs for surface spectroscopy. The lateral extent of electromagnetic propagation along the mesh surface is measured by recording absorption spectra of a line of latex microspheres as a function of distance away from the line along the mesh. Measurements reveal an exponential functional form for decay of absorption signal laterally from the absorption source. Results at 697 cm^{-1} , which are closest to the strongest transmission resonance of the mesh, reveal a $1/e$ propagation distance along the surface of $17.8 \pm 2.9\ \mu\text{m}$. This is 40% larger than the lattice spacing implicating the holes as the SPP damping mechanism, however, this is significantly shorter than smooth metal expectations. © 2009 American Institute of Physics. [DOI: 10.1063/1.3204693]

I. INTRODUCTION

An optically thick, smooth metal film transmits radiation efficiently upon perforation with an array of subwavelength holes.¹⁻³ These constructions have been called inductive grids⁴ or meshes and demonstrate unusual optical properties^{1,5-7} including the extraordinary transmission effect.^{1,2} More radiation can be transmitted by the mesh than is incident upon its holes, i.e., light that initially hits metal runs laterally along the surface of the mesh until re-emission at a hole. This effect is attributed to a role of surface plasmon polaritons^{1,2,7-10} (SPPs, a mixed state between light and the conducting electrons of the metal) and has garnered much interest and some debate. Distinctions can be made about whether the polaritons are more lightlike or more like waves of surface electrons; however, all of these phenomena are discussed in the recent literature under the heading of surface plasmons (SPs), and we will do the same. To be clear, the SPs in this work are very lightlike, i.e., more like light trapped at the surface of a metal by interaction with metallic conducting electrons rather than surface electron waves. In this work, measurements are made of the propagation length along the surface of the mesh, which is at a very different angle than the incident beam, using infrared (IR) absorption spectroscopy. The IR SP nature of the subject metal meshes has been well documented^{2,10-12} primarily regarding the positions of transmission resonances. There is some work on the widths and/or lifetimes of these resonances^{2,12} and these results will be considered relative to the presently described measurements of propagation lengths.

Metal films with arrays of subwavelength holes are considered to be new plasmonic metamaterials.^{13,14} Recent

reviews exist on mesh plasmonics and its applications,^{11,15} including one of our own work,¹² which pushes extraordinary transmission into the mid-IR region to overlap with the vibrational spectra of molecules on mesh. Interest in both local and propagating SPs^{7,16,17} exists because they exhibit high electric fields at the surface of the metal¹⁸ for supersensitive surface enhanced Raman spectroscopy,¹⁹ reduced wavelengths relative to the incident radiation for subwavelength optics^{5,7,20} and near field scanning optical microscopy,²¹ increased transmission to facilitate superlensing¹⁴ and more sensitive absorption spectroscopy,²² confinement to two dimensions⁹ to advance the probing of subwavelength nanospaces, potential for bridging photonics and electronics (plasmonics²³), sensitivity as sensors¹⁷ for bioanalytical assays with SP attenuated total reflection, and more efficient collection of fluorescence²⁴ using SP coupled emission. All of the above are due in large part to SP-mediated optical properties.

Doubts about the role of SPs in extraordinary transmission of mesh arrays arose significantly with the work of Lezec and Thio,²⁵ but their reservations and model have been largely rebuffed.^{26,27} Unexpected attenuation of radiation between slits of subwavelength holes²⁵ was alleviated by the use of coherent laser sources and now these experiments suggest a role for SPs.²⁸ Some did not like the larger shifts of resonance positions from zero-order, smooth metal predictions, however, these are now understood as due to coupling of SPs between the front and back surfaces of the mesh through the holes.^{10-12,29} One can also observe transmission resonances due to modes other than SPs for “bad” SP metals [such as Cr,³⁰ W,^{25,31} and Si (Ref. 32)], but coupling to SP modes of metals gives much greater resonance intensity. Calculations^{13,33,34} show that meshes of perfect metals

^{a)}Electronic mail: coe.1@osu.edu.

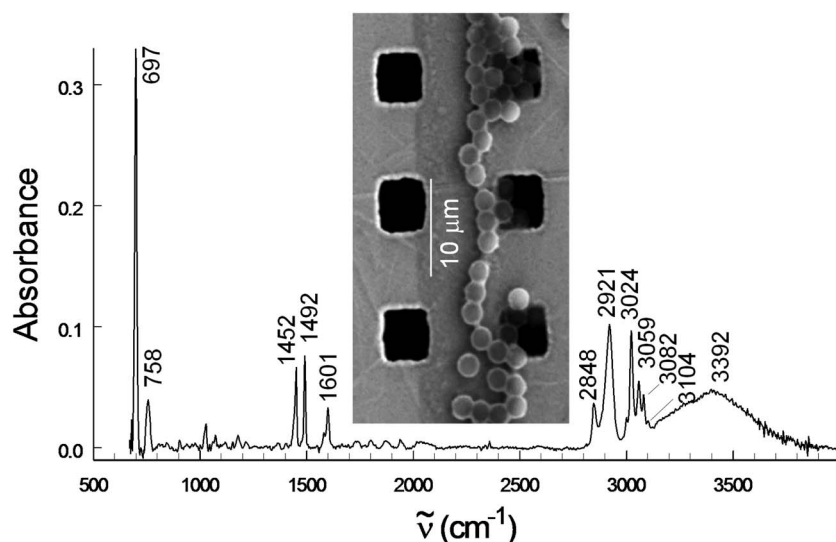


FIG. 1. IR absorption spectrum of a line of $2 \mu\text{m}$ diameter latex (polystyrene) spheres on a Ni mesh showing the most prominent vibrational bands. Inset is a SEM image of a region similar to that associated with the IR spectrum.

exhibit transmission resonances and bound surface waves even though smooth perfect metals do not support SPs. Clearly the holes or geometry of mesh can contribute to coupling or damping of SPs, i.e., to the imaginary component of the SP wavevector parallel to the surface of the structured system, which stands in contrast with a smooth metal interface where the intrinsic value depends only on the complex dielectric “constant” of the metal and substrate. Finally, different classifications of SP-like states, such as surface states³⁵ and “spoof” plasmons³³ may be useful and these issues are still being sorted out.

Propagation lengths of SPs can be measured with a variety of techniques, including near-field scanning optical microscopy^{27,36} and cathode luminescence.³⁷ These and related techniques run into challenges as they approach the IR region. The first SP propagation measurement in the IR was made in 1973 by Schoenwald *et al.*³⁸ and Zhizhin *et al.*³⁹ using a pair of prism couplers. CO₂ laser light (at the appropriate angle) was prism coupled into the nonleaky SP mode of a smooth air/metal interface, which propagated for a distance until light was coupled out with a second prism. Plots of output intensity versus distance between the prisms yield $1/e$ propagation constants. Furthermore with molecules at the air/metal interface, such sequences of measurements could be repeated at different frequencies (subject to the limited tunability of high power CO₂ lasers) yielding absorption spectra of the molecules^{39,40} in plots of $1/e$ propagation length versus frequency. This was a lot of work, but piques interest in using SP phenomena to obtain molecular vibrational spectra. How do SP properties manifest themselves in systems better attuned to acquiring vibrational spectra? Since a Fourier transform IR (FTIR) microscopic imaging spectrometer could use metal microarrays to access SPs, how would the incoherent IR source and the spread of k values influence the results? In this work, spectroscopic measurements are made at a range of wavelengths throughout the mid-IR region with regard to how far the probing radiation (SPs) runs laterally along the surface of such arrays.

II. IR IMAGING EXPERIMENT

Latex (polystyrene) microspheres were chosen as the sample in these experiments because they have vibrational features throughout the mid-IR region and they can be arranged in space on the microscale. There is in fact a growing body of work in nanotechnology using micro- and nanospheres as carriers of drug molecules,⁴¹ as microlasers,⁴² as well as substrates for reactions giving nano-/microscale constructions,⁴³ such as metal nanoshells.⁴⁴ In this work, experiments were accomplished using polystyrene microspheres from Duke Scientific (Surf-Cal PD2000, $2.01 \pm 0.04 \mu\text{m}$ diameter in de-ionized filtered water, 3×10^8 particles/ml, $n=1.59$ at 589 nm). The samples were prepared by evaporation of a small drop of the commercial suspension on Ni photonic mesh (Precision Eforming, $12.6 \mu\text{m}$ square lattice parameter, $5.5 \mu\text{m}$ square holes, $\sim 2 \mu\text{m}$ thickness) leaving a macroscopic ring of microspheres on the surface from the edge of the drop. After drying, a drop of distilled water was applied without any agitation to dissolve any surfactant and the drop was removed with a corner of a Kimwipe™. A scanning electron microscope (SEM) image of a portion of the resulting ring, although not the exact region probed spectroscopically, is shown in the inset of Fig. 1 as recorded with a JEOL JSM-5500 instrument. In a microscopic region, one obtains a line of microspheres (both in and out of holes) and experiments proceed by measuring the IR absorption spectrum of the polystyrene as a function of distance from the line of microspheres. An IR absorption spectrum (flattened baseline) from a region directly over the line of latex microspheres is shown in Fig. 1. Each vibrational band represents a wavelength at which lateral propagation of light can be investigated.

IR transmission spectra of a $125 \times 37.5 \mu\text{m}^2$ region including a line of $2 \mu\text{m}$ diameter latex microspheres were recorded in the imaging mode of a FTIR microscope (Perkin Elmer Spectrum Spotlight 300 with a Cassegrain optical system, numerical aperture=0.6). An optical image of this region is shown at the bottom of Fig. 2. The blackened region is the line of latex microspheres and the white dotted line shows the position of the pixels closest to the end of the latex

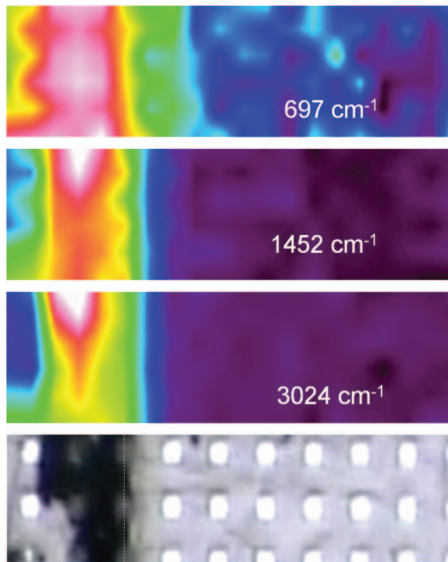


FIG. 2. Bottom: optical microscope image of the line region of 2 μm diameter latex (polystyrene) spheres on a Ni mesh as recorded with an IR microspectrometer (Perkin Elmer Spectrum Spotlight 300). The dark region is the line of microspheres. Top three panels are images due to IR absorption at the specified wavenumbers and correspond spatially to the bottom optical image. As wavenumbers get smaller, absorption can be detected laterally further from the absorbing source, the line of latex microspheres.

microsphere sample. Spectra were recorded at 4 cm^{-1} resolution, with 256 scans, at 6.25 $\mu\text{m}/\text{pixel}$ using a 16 detector array of liquid nitrogen-cooled HgCdTe elements, requiring 80 min of acquisition time, using a region of mesh absent of latex microspheres as background. The result was a transmission spectrum from 670 to 4000 cm^{-1} at each point in a square grid of 6.25 μm pixel size, i.e., 120 spectra, each from a point on a 20 pixel by 6 pixel grid within the image region. The software allows one to extract absorbances of specific vibrational features over the image grid by choosing two points at nearby frequencies that define a baseline for a peak maximum at a specified frequency. The top three panels of Fig. 2 are contour absorbance plots at 697, 1452, and 3024 cm^{-1} corresponding to the bottom optical image. Clearly, absorption extends further into the bare mesh region as the frequency gets smaller.

III. IR IMAGING RESULTS FOR PROPAGATION LENGTHS

Since results depend on the ability to make measurements in regions of exponentially decaying signal, the imaging regions have been oriented so that averaging may be employed vertically, parallel to the line of microspheres. Averages of absorbance over the six vertical pixels are displayed at selected frequencies of vibrational bands of polystyrene microspheres in Fig. 3. Each point in the plots of Fig. 3 corresponds to $6 \times 256 = 1536$ scans. The absorbance data were fitted with a nonlinear least-squares program to obtain the α_0 and α_1 parameters of the following exponential form:

$$\alpha_0 e^{-x/\alpha_1} + \alpha_2, \quad (1)$$

where x is distance from the end of the microsphere line, α_0 is the intensity of absorption, α_1 is the 1/e propagation dis-

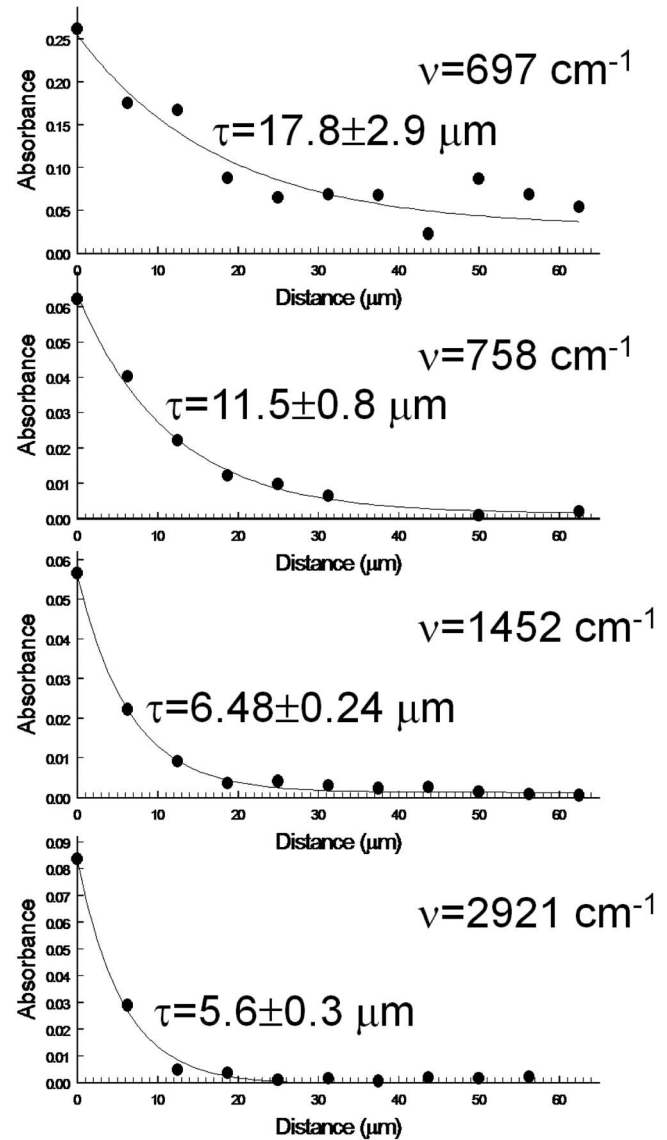


FIG. 3. Absorbance as a function of lateral distance along the mesh away from a line of 2 μm diameter microspheres at specific wavenumbers (ν). The data have been nonlinearly fit to an exponential function (solid lines) in order to determine 1/e propagation distances (τ) that are given on each trace and at various other wavenumbers in Table I.

tance, and α_2 is an offset determined by averaging the four most distant points in the image from the line accounting for imperfections in the background. The resulting fit curves are given graphically for selected vibrations in Fig. 3 and the numerical parameters are given at all available vibrational frequencies in Table I. The data fit very well to an exponential function, particularly at the smaller vibrational frequencies—even though three or so holes occupy the space spanned by these measurements. However, other functions, such as a Gaussian, have comparable (and sometimes marginally better) fits at the larger vibrational frequencies (shorter wavelengths). In fact, at wavelengths shorter than the pixel size, it can be expected that the details of the microsphere arrangement become important and should be rigorously convolved with the exponential function of lateral propagation.

On this mesh, the smallest frequencies have the largest

TABLE I. Nonlinear least-squares fitting parameters as given in Eq. (1). The $1/e$ propagation distance is given by the parameter α_1 .

$\tilde{\nu}$ (cm^{-1})	α_0 (absorbance units)	α_1 (μm)	α_2 (absorbance units)
697	0.225 ± 0.022	17.8 ± 2.9	0.0303
758	0.0621 ± 0.0022	11.5 ± 0.8	1.43×10^{-3}
1452	0.0551 ± 0.0009	6.48 ± 0.24	1.32×10^{-3}
1492	0.0630 ± 0.0016	7.4 ± 0.4	4.36×10^{-4}
1601	0.0279 ± 0.0012	6.8 ± 0.6	3.17×10^{-4}
2848	0.0309 ± 0.0020	6.9 ± 0.9	-5.25×10^{-5}
2921	0.0844 ± 0.0021	5.6 ± 0.3	-6.00×10^{-4}
3024	0.0749 ± 0.0017	5.9 ± 0.4	2.70×10^{-4}
3059	0.0376 ± 0.0005	6.0 ± 0.3	-9.75×10^{-6}
3082	0.0252 ± 0.0015	5.8 ± 0.8	1.23×10^{-4}
3104	0.0066 ± 0.0007	5.0 ± 1.4	5.63×10^{-4}
3392	0.033 ± 0.010	5.4 ± 3.7	9.60×10^{-3}

$1/e$ propagation distances. At 697 cm^{-1} , the $1/e$ propagation distance is $17.8 \mu\text{m}$, which is larger than the $7 \mu\text{m}$ of metal between holes, the $12.6 \mu\text{m}$ lattice parameter (hole-center-to-hole-center distance), and the $14.3 \mu\text{m}$ wavelength of the incident light. The 697 cm^{-1} frequency is close to the strongest transmission resonance on this mesh,^{10–12,29} which occurs at 749 cm^{-1} at perpendicular incidence ($k_x=0$). The Cassegrain optical system of the FTIR microspectrometer does not transmit rays on the optical axis. It transmits angles nominally from 21° – 37° cylindrically off of the optical centerline, with the smaller angles having more intensity. The frequency of the 697 cm^{-1} vibration lies between the k -space dispersion curves of the $(-1,0)$ and $(0, \pm 1)$ resonances in the ΓX geometry and near the $(-1,0)$ and $(0,-1)$ resonances in the ΓM direction. It does not optimally overlap with any of these, but all of these resonances are sufficiently wide that there is some overlap. From one preliminary experiment (Rodriguez), a $1/e$ propagation distance of $27 \mu\text{m}$ was obtained by tilting the mesh by 13° relative to the surface of the microscope stage. So we suspect that one can do better with tilting compared to the present flat results. Also, note that the data in Fig. 3 are noisiest at 697 cm^{-1} because the instrument's specified range ends at 720 cm^{-1} , i.e., there is diminishing light and higher noise at 697 cm^{-1} .

IV. CONCLUSION

At 697 cm^{-1} , which is closest to the most intense SP resonance, the principle results are a single exponential distribution with a $1/e$ propagation constant of $17.8 \pm 2.9 \mu\text{m}$. Expectations about these results come from the theory of SP damping at smooth metal interfaces,⁴⁵ which predicts exponential damping due to factors such as the intrinsic mechanism (from the complex dielectric constants of the metal and substrate), as well as scattering from surface roughness. Using a complex dielectric “constant”⁴⁶ for Ni metal of $-2378 + i1481$ at 697 cm^{-1} , an intrinsic $1/e$ propagation distance of 8.7 mm is predicted. While the observed value is a factor of ~ 480 times shorter than the intrinsic value, note that the observed value is still larger than the mesh lattice parameter ($12.6 \mu\text{m}$), larger than the wavelength ($697 \text{ cm}^{-1} \rightarrow 14.3 \mu\text{m}$), and the corresponding transmission

resonances still disperse like SPs. Unlike smooth metal surfaces, the SPs on mesh have more complicated options, including lateral reflection or transmission at holes (on the front and back side of the mesh), as well as output in the forward or backward direction at holes. For this reason, it was not at all clear that a simple exponential would be obtained as the attenuation function. The single exponential result provides evidence for the mesh acting as an effective medium at wavelengths larger than the lattice parameter, with a single dominant damping mechanism—the holes (as opposed to other possible alternatives such as surface roughness).

The present results can be compared to previous work² on similar metal meshes, which offered a formula predicting a resonance linewidth of 67 cm^{-1} at a frequency of 697 cm^{-1} corresponding to a propagation distance of $22 \mu\text{m}$ (at 94% of c), which is in reasonable agreement with the present measurement of $17.8 \pm 2.9 \mu\text{m}$. This suggests that lateral SP propagation with damping at holes is the same phenomenon that gives rise to the width (or lifetime) of the transmission resonances. The holes are strong damping units with the majority of SP damping occurring in the region of the first hole and a bit less at the second. Note that damping at mesh holes causes loss of SPs but does not necessarily result in loss of photons from the emerging photon beam, i.e., perforated mesh is also a good output coupler. The currently measured propagation length at 697 cm^{-1} corresponds to a k'' value (imaginary part of the SP wavevector parallel to the surface) of 281 cm^{-1} using the relation that propagation length equals $1/(2k'')$. Such measurements should be useful to the development of theoretical models for metal films with arrays of holes (as are available for smooth metal interfaces).

Our ultimate motivation for this study concerns the expectation that large SP lateral propagation distances would give rise to large absorption path lengths. However, if lateral propagation was important (particularly at the longest spectral wavelengths), then we should observe large enhancements in the intensity of the peak at 697 cm^{-1} relative to the other peaks in the absorption spectrum. Enhancements due to lateral propagation along the surface are only of the order of a factor of ~ 3 . This mechanism is not responsible for most of the IR absorption enhancements reported by us.^{11,12} Apparently, whether material is inside or out of the microholes is much more important for spectroscopic enhancements and the subject of a following paper.

ACKNOWLEDGMENTS

We thank the National Science Foundation for support of this work under Grant Nos. CHE 0848486 and CHE-0639163.

¹T. W. Ebbesen, H. J. Lezec, H. F. Ghaemi, T. Thio, and P. A. Wolff, *Nature (London)* **391**, 667 (1998).

²S. M. Williams, A. D. Stafford, K. R. Rodriguez, T. M. Rogers, and J. V. Coe, *J. Phys. Chem. B* **107**, 11871 (2003).

³K. D. Moller, K. R. Farmer, D. V. P. Ivanov, O. Sternberg, K. P. Stewart, and P. Lalanne, *Infrared Phys. Technol.* **40**, 475 (1999); R. Ulrich, “Modes of Propagation on an Open Periodic Waveguide for the Far

- Infrared*," in Proceedings of the Symposium on Optical and Acoustical Microelectronics, New York, NY, April 16–18, 1974 (Polytechnic Press, New York, 1975).
- ⁴R. Ulrich, *Infrared Phys.* **7**, 37 (1967); R. C. McPhedran and D. Maystre, *Appl. Phys. (Berlin)* **14**, 1 (1977); B. K. Minhas, W. Fan, K. Agi, S. R. J. Brueck, and K. J. Malloy, *J. Opt. Soc. Am. A Opt. Image Sci. Vis.* **19**, 1352 (2002).
- ⁵W. L. Barnes, A. Dereux, and T. W. Ebbesen, *Nature (London)* **424**, 824 (2003).
- ⁶J. Dintinger, A. Degiron, and T. W. Ebbesen, *MRS Bull.* **30**, 381 (2005).
- ⁷C. Genet and T. W. Ebbesen, *Nature (London)* **445**, 39 (2007).
- ⁸W. L. Barnes, W. A. Murray, J. Dintinger, E. Devaux, and T. W. Ebbesen, *Phys. Rev. Lett.* **92**, 107401 (2004).
- ⁹S. Teeters-Kennedy, Ph.D. Infrared Surface Plasmons in Double Stacked Nickel Microarrays: Lipid Bilayer Systems, The Ohio State University (2007).
- ¹⁰S. M. Williams and J. V. Coe, *Plasmonics* **1**, 87 (2006).
- ¹¹J. V. Coe, J. M. Heer, S. Teeters-Kennedy, H. Tian, and K. R. Rodriguez, *Annu. Rev. Phys. Chem.* **59**, 179 (2008).
- ¹²J. V. Coe, K. R. Rodriguez, S. Teeters-Kennedy, K. Cilwa, J. Heer, H. Tian, and S. M. Williams, *J. Phys. Chem. C* **111**, 17459 (2007).
- ¹³F. J. Garcia-Vidal, L. Martin-Moreno, and J. B. Pendry, *J. Opt. A, Pure Appl. Opt.* **7**, S97 (2005).
- ¹⁴N. Fang, Z. Liu, T.-J. Yen, and X. Zhang, *Opt. Express* **11**, 682 (2003); N. Fang and X. Zhang, *Appl. Phys. Lett.* **82**, 161 (2003).
- ¹⁵R. Gordon, D. Sinton, K. Kavanagh, and A. G. Brolo, *Acc. Chem. Res.* **41**, 1049 (2008).
- ¹⁶K. A. Willets and R. P. V. Duyne, *Annu. Rev. Phys. Chem.* **58**, 267 (2007); P. C. Andersen and K. L. Rowlen, *Appl. Spectrosc.* **56**, 124A (2002).
- ¹⁷A. J. Haes and R. P. Van Duyne, *Anal. Bioanal. Chem.* **379**, 920 (2004).
- ¹⁸N. E. Glass, A. A. Maradudin, and V. Celli, *Phys. Rev. B* **27**, 5150 (1983); K. Kneipp, H. Kneipp, R. Manoharan, E. B. Hanlon, I. Itzkan, R. R. Dasari, and M. S. Feld, *Appl. Spectrosc.* **52**, 1493 (1998); A. G. Brolo, E. Arctander, R. Gordon, B. Leathem, and K. Kavanagh, *Nano Lett.* **4**, 2015 (2004).
- ¹⁹E. A. Batista, D. P. dos Santos, G. F. S. Andrade, A. C. Sant'Ana, A. G. Brolo, and M. L. A. Temperini, *J. Nanosci. Nanotechnol.* **9**, 3233 (2009); S. Nie and S. R. Emory, *Science* **275**, 1102 (1997); K. Kneipp, Y. Wang, H. Kneipp, L. T. Perelman, I. Itzkan, R. R. Dasari, and M. S. Feld, *Phys. Rev. Lett.* **78**, 1667 (1997).
- ²⁰N. Fang, H. Lee, C. Sun, and X. Zhang, *Science* **308**, 534 (2005); A. Degiron, H. J. Lezec, N. Yamamoto, and T. W. Ebbesen, *Opt. Commun.* **239**, 61 (2004); D. Zhang, P. Wang, X. Jiao, L. Tang, Y. Lu, and H. Ming, *Wuli* **34**, 508 (2005); L. Martin-Moreno and F. J. Garcia-Vidal, *Adv. Solid State Phys.* **44**, 69 (2004); S. A. Maier, *IEEE J. Sel. Top. Quantum Electron.* **12**, 1214 (2006); S. A. Maier, M. L. Brongersma, P. G. Kik, S. Meltzer, A. A. G. Requicha, and H. A. Atwater, *Adv. Mater. (Weinheim, Ger.)* **13**, 1501 (2001); S. A. Maier, *Current Nanoscience* **1**, 17 (2005).
- ²¹L. Yin, V. K. Vlasko-Vlasov, A. Rydh, J. Pearson, U. Welp, S.-H. Chang, S. K. Gray, G. C. Schatz, D. B. Brown, and C. W. Kimball, *Appl. Phys. Lett.* **85**, 467 (2004).
- ²²K. R. Rodriguez, S. Shah, S. M. Williams, S. Teeters-Kennedy, and J. V. Coe, *J. Chem. Phys.* **121**, 8671 (2004).
- ²³E. Ozbay, *Science* **311**, 189 (2006).
- ²⁴J. R. Lakowicz, *Anal. Biochem.* **324**, 153 (2004); A. G. Brolo, S. C. Kwok, M. G. Moffitt, R. Gordon, J. Riordon, and K. L. Kavanagh, *J. Am. Chem. Soc.* **127**, 14936 (2005).
- ²⁵H. J. Lezec and T. Thio, *Opt. Express* **12**, 3629 (2004).
- ²⁶F. J. Garcia-Vidal, S. G. Rodrigo, and L. Martin-Moreno, *Nat. Phys.* **2**, 790 (2006); P. Lalanne and J. P. Hugonin, *ibid.* **2**, 551 (2006); L. Chen, J. T. Robinson, and M. Lipson, *Opt. Express* **14**, 12629 (2006).
- ²⁷H. W. Gao, J. Henzie, and T. W. Odom, *Nano Lett.* **6**, 2104 (2006).
- ²⁸G. Gay, O. Alloschery, B. Viaris de Lesegno, C. O'Dwyer, J. Weiner, and H. J. Lezec, *Nat. Phys.* **2**, 262 (2006).
- ²⁹S. M. Williams, A. D. Stafford, T. M. Rogers, S. R. Bishop, and J. V. Coe, *Appl. Phys. Lett.* **85**, 1472 (2004); S. Teeters-Kennedy, S. M. Williams, K. R. Rodriguez, K. Cilwa, D. Meleason, A. Sudnitsyn, F. Hrovat, and J. V. Coe, *J. Phys. Chem. C* **111**, 124 (2007); J. V. Coe, S. M. Williams, K. Rodriguez, R. S. Teeters-Kennedy, A. Sudnitsyn, and F. Hrovat, *Anal. Chem.* **78**, 1384 (2006).
- ³⁰T. Thio, H. F. Ghaemi, H. J. Lezec, P. A. Wolff, and T. W. Ebbesen, *J. Opt. Soc. Am. B* **16**, 1743 (1999); M. Sarrazin and J.-P. Vigneron, *Phys. Rev. B* **71**, 075404 (2005).
- ³¹M. Sarrazin and J.-P. Vigneron, *Phys. Rev. E* **68**, 016603 (2003).
- ³²D. E. Grupp, H. J. Lezec, T. W. Ebbesen, K. M. Pellerin, and T. Thio, *Appl. Phys. Lett.* **77**, 1569 (2000).
- ³³J. B. Pendry, L. Martin-Moreno, and F. J. Garcia-Vidal, *Science* **305**, 847 (2004).
- ³⁴J. Bravo-Abad, F. J. Garcia-Vidal, and L. Martin-Moreno, *Phys. Rev. Lett.* **93**, 227401 (2004); S. Selcuk, K. Woo, D. B. Tanner, A. F. Hebard, A. G. Borisov, and S. V. Shabanov, *ibid.* **97**, 067403 (2006); V. Lomakin and E. Michielssen, *Phys. Rev. B* **71**, 235117 (2005); T. Tanaka, M. Akazawa, E. Sano, M. Tanaka, F. Miyamaru, and M. Hangyo, *Jpn. J. Appl. Phys., Part 1* **45**, 4058 (2006); J. Bravo-Abad, L. Martin-Moreno, and F. J. Garcia-Vidal, *IEEE J. Sel. Top. Quantum Electron.* **12**, 1221 (2006).
- ³⁵J. B. Pendry, NATO ASI Ser., Ser. C **C73**, 1 (1981).
- ³⁶J. Y. Lalue, E. Devaux, C. Genet, T. W. Ebbesen, J. C. Weeber, and A. Dereux, *Opt. Express* **15**, 3488 (2007); E.-S. Kwak, J. Henzie, S.-H. Chang, K. Gray Stephen, C. Schatz George, and W. Odom Teri, *Nano Lett.* **5**, 1963 (2005); B. Hecht, H. Bielefeldt, L. Novotny, Y. Inouye, and D. W. Pohl, *Phys. Rev. Lett.* **77**, 1889 (1996); J. P. Thost, W. Krieger, N. Kroo, Z. Szentirmay, and H. Walther, *Opt. Commun.* **103**, 194 (1993); M. Specht, J. Pedarnig, W. Heckl, and T. Haensch, *Phys. Unserer Zeit* **24**, 176 (1993).
- ³⁷M. Kuttge, E. J. R. Vesseur, J. Verhoeven, H. J. Lezec, H. A. Atwater, and A. Polman, *Appl. Phys. Lett.* **93**, 113110 (2008); J. T. van Wijngaarden, E. Verhagen, A. Polman, C. E. Ross, H. J. Lezec, and H. A. Atwater, *ibid.* **88**, 221111 (2006).
- ³⁸J. Schoenwald, E. Burstein, and J. Elson, *Solid State Commun.* **12**, 185 (1973).
- ³⁹G. N. Zhizhin, E. A. Vinogradov, M. A. Moskalova, and V. A. Yakovlev, *Appl. Spectrosc. Rev.* **18**, 171 (1982–83).
- ⁴⁰G. N. Zhizhin, M. A. Moskalova, E. A. Vinogradov, A. A. Sigarev, and V. A. Yakovlev, *J. Electron Spectrosc. Relat. Phenom.* **30**, 35 (1983); V. I. Silin, S. A. Voronov, V. A. Yakovlev, and G. N. Zhizhin, *Int. J. Infrared Millim. Waves* **10**, 101 (1989); E. V. Alieva, G. Beitel, L. A. Kuzik, A. A. Sigarev, V. A. Yakovlev, G. N. Zhizhin, A. F. G. d. Meer, and M. J. d. Wiel, *Appl. Spectrosc.* **51**, 584 (1997).
- ⁴¹M. Saravanan, K. Bhaskar, G. S. Rao, and M. D. Dhanaraju, *J. Microencapsul.* **20**, 289 (2003); K. S. Soppimath, T. M. Aminabhavi, A. R. Kulkarni, and W. E. Rudzinski, *J. Controlled Release* **70**, 1 (2001); D. T. O'Hagan, *Adv. Drug Delivery Rev.* **34**, 305 (1998).
- ⁴²T. Benson, S. Boriskina, P. Sewell, A. Vukovic, S. Greedy, and A. Nosich, *Frontiers in Planar Lightwave Circuit Technology* (Springer, The Netherlands, 2006), p. 39.
- ⁴³Q. Ma, T. Y. Song, X. Y. Wang, Y. B. Li, Y. H. Shi, and X. G. Su, *Spectrosc. Lett.* **40**, 113 (2007).
- ⁴⁴K. T. Yong, Y. Sahoo, M. T. Swihart, and P. N. Prasad, *Colloids Surf., A* **290**, 89 (2006); W. L. Shi, Y. Sahoo, M. T. Swihart, and P. N. Prasad, *Langmuir* **21**, 1610 (2005).
- ⁴⁵H. Raether, *Surface Plasmons on Smooth and Rough Surfaces and on Gratings* (Springer-Verlag, Berlin, 1988).
- ⁴⁶A. D. Rakic, A. B. Djuricic, J. M. Elazar, and M. L. Majewski, *Appl. Opt.* **37**, 5271 (1998).